BRAIN
A JOURNAL OF NEUROLOGY

Side population in human glioblastoma is non-tumorigenic and characterizes brain endothelial cells

Anna Golebiewska,[1] Sébastien Bougnaud,[1] Daniel Stieber,[1] Nicolaas H. C. Brons,[2] Laurent Vallar,[3] Frank Hertel,[4] Barbara Klink,[5] Evelin Schröck,[5] Rolf Bjerkvig[1,6] and Simone P. Niclou[1]

1 NorLux Neuro-Oncology Laboratory, Department of Oncology, Centre de Recherche Public de la Santé (CRP-Santé), L-1526 Luxembourg, Luxembourg
2 Core Facility Flow Cytometry, Centre de Recherche Public de la Santé (CRP-Santé), L-1526 Luxembourg, Luxembourg
3 Genomics Research Unit, Centre de Recherche Public de la Santé (CRP-Santé), L-1526 Luxembourg, Luxembourg
4 Centre Hospitalier Luxembourg, Department of Neurosurgery, L-1210 Luxembourg, Luxembourg
5 Institute for Clincial Genetics, Technical University Dresden, 01307 Dresden, Germany
6 NorLux Neuro-Oncology, Department of Biomedicine, University of Bergen, N-5009 Bergen, Norway

Correspondence to: Simone P. Niclou, PhD
Centre de Recherche Public de la Santé (CRP-Santé)
Department of Oncology
NorLux Neuro-Oncology Laboratory
84, Val Fleuri, L- 1526
Luxembourg
E-mail: simone.niclou@crp-sante.lu

The identification and significance of cancer stem-like cells in malignant gliomas remains controversial. It has been proposed that cancer stem-like cells display increased drug resistance, through the expression of ATP-binding cassette transporters that detoxify cells by effluxing exogenous compounds. Here, we investigated the 'side population' phenotype based on efflux properties of ATP-binding cassette transporters in freshly isolated human glioblastoma samples and intracranial xenografts derived thereof. Using fluorescence *in situ* hybridization analysis on sorted cells obtained from glioblastoma biopsies, as well as human tumour xenografts developed in immunodeficient enhanced green fluorescence protein-expressing mice that allow an unequivocal tumour-stroma discrimination, we show that side population cells in human glioblastoma are non-neoplastic and exclusively stroma-derived. Tumour cells were consistently devoid of efflux properties regardless of their genetic background, tumour ploidy or stem cell associated marker expression. Using multi-parameter flow cytometry we identified the stromal side population in human glioblastoma to be brain-derived endothelial cells with a minor contribution of astrocytes. In contrast with their foetal counterpart, neural stem/progenitor cells in the adult brain did not display the side population phenotype. Of note, we show that CD133-positive cells often associated with cancer stem-like cells in glioblastoma biopsies, do not represent a homogenous cell population and include CD31-positive endothelial cells. Interestingly, treatment of brain tumours with the anti-angiogenic agent bevacizumab reduced total vessel density, but did not affect the efflux properties of endothelial cells. In conclusion our findings contribute to an unbiased identification of cancer stem-like cells and stromal cells in brain neoplasms, and provide novel insight into the complex issue of drug delivery to the brain. Since efflux properties of endothelial cells are likely to compromise drug availability, transiently targeting ATP-binding cassette transporters may be a valuable therapeutic strategy to improve treatment effects in brain tumours.

Introduction

Glioblastoma multiforme, a grade IV glioma is a deadly tumour for which no curative treatment is available. Typical features of glioblastoma include aggressive proliferation, a strong invasive capacity and extensive angiogenesis within the tumour core. Moreover glioblastoma is known as a highly heterogeneous tumour, both at the cellular and genetic level. Like many solid tumours, brain tumours contain not only neoplastic cells but also a variety of stromal cells. More recently glioblastoma has been proposed to be maintained by a subset of undifferentiated neoplastic cells, so called 'cancer stem cells' that are thought to drive tumour progression and recurrence (Singh et al., 2003, 2004). Cancer stem cells are defined by an increased tumorigenic potential upon xenotransplantation, long-term self-renewal capacity in vitro, a multipotent differentiation capacity and strong resistance to therapy (Park and Rich, 2009). Glioblastoma stem-like cells are generally identified based on their expression of cell surface markers or based on their growth potential as non-adherent neurospheres in defined medium (Singh et al., 2004; Ogden et al., 2008; Son et al., 2009; Anido et al., 2010). Despite the fact that several putative glioblastoma stem cell markers including CD133, CD15, CD44 or A2B5 are extensively used for their identification, there is still a considerable debate on how to reliably identify and isolate cancer stem-like cells in gliomas (Wang et al., 2008; Chen et al., 2010; Barrett et al., 2012).

Because cancer stem-like cells are thought to be responsible for disease recurrence due to increased chemoresistance, we hypothesized that the ATP-binding cassette (ABC) transporters could represent a prominent functional marker for glioblastoma stem-like cells. ABC transporters belong to a superfamily of membrane pumps that catalyse the ATP-dependent transport of various endogenous compounds and xenobiotics out of the cell. The best characterized family members ABCB1 (also known as MDR1 and p-glycoprotein) and ABCG2 (also known as BCRP1) (Zhou et al., 2001; Patrawala et al., 2005) are responsible for the so-called 'side population' phenotype, originally described in bone marrow stem cells (Goodell et al., 1996). The side population discrimination assay relies on the capacity of metabolically active cells to differentially efflux fluorescent dyes (Golebiewska et al., 2011) and has been instrumental to identify stem and progenitor cell populations in normal tissues (Challen and Little, 2006). Moreover, side population cells were identified in certain malignancies including neuroblastomas (Hirschmann-Jax et al., 2004), breast cancer (Patrawala et al., 2005), ovarian cancer (Szotek et al., 2006) and various mesenchymal neoplasms (Wu et al., 2007), where they were found to have improved clonogenic and tumorigenic potential and higher chemoresistance compared with non-side population cells. For malignant gliomas, there is conflicting data in the literature with regard to the presence of the side population phenotype, e.g. while efflux properties in glioma cell lines have been described in some reports

(Hirschmann-Jax et al., 2004; Seidel et al., 2010), they were not confirmed in others (Broadley et al., 2011; Golebiewska et al., 2011). Moreover the side population phenotype has been characterized in putative glioma stem-like cells isolated from a transgenic mouse model (Bleau et al., 2009); however, no in vivo data are currently available from patient-derived gliomas. This question is particularly important since long term culture can influence dye efflux properties (Torok et al., 2003), thus the nature and identity of the side population phenotype in human brain cancer remains elusive (Beier et al., 2011; Tang, 2012).

It should be emphasized that the side population phenotype is neither specific nor universal for stem cells. In particular in the normal brain, ABC transporters are expressed in capillary endothelial cells where they protect neural tissue from blood-derived molecules thereby contributing to a functional blood–brain barrier (Schinkel, 1999). This represents a major impediment in brain disorders as endothelial membrane pumps severely restrict drug delivery to the brain parenchyma (Agarwal et al., 2011). Anatomically the neurovascular unit consists of different cell types including microvascular endothelial cells, pericytes and perivascular astrocytes, where endothelial cells and astrocytic end-feet express ABC transporters (Bernacki et al., 2008). In glioblastoma the blood–brain barrier is disrupted in the tumour core, which is characterized by aberrant vessel morphology and vessel leakiness. The invasive component of the tumour is, however, largely protected from circulating drugs by an intact blood–brain barrier (Carmeliet and Jain, 2011). There is currently little known about efflux properties within glioma vessels. Another unresolved question is whether and how anti-angiogenic agents influence the efflux properties of tumour endothelial cells, and whether a 'normalized' vasculature is more or less selective for drug penetration (Agarwal et al., 2011).

In this study we provide a detailed phenotypic and functional characterization of the side population phenotype and of tumour stroma, including brain endothelial cells, in fresh human glioblastoma biopsies and in clinically relevant patient derived xenografts.

Materials and methods

Patient-derived brain tumours

Human glioblastoma biopsies were obtained from the Neurosurgery Department of the Centre Hospitalier in Luxembourg (CHL) or the Department of Neurosurgery, Haukeland University Hospital in Bergen, Norway. All patients had provided informed consent and tumour collection and analysis was approved by the National Research Ethics Committee for Luxembourg (CNER) or by the Regional Ethical Board at the Haukeland University Hospital in Bergen. All biopsies were primary glioblastomas based on neuropathological diagnosis and genomic analysis by array comparative genomic hybridization (see Supplementary Table 1 for clinical details and genomic profiles).

Orthotopic biopsy-derived glioblastoma xenografts

Organotypic glioblastoma spheroids from patient samples were prepared as previously described (Keunen *et al.*, 2011) and maintained in spheroid medium [Dulbecco's modified Eagle medium (Lonza), 10% foetal bovine serum (Lonza), 2 mM L-glutamine, 0.4 mM non-essential amino acid and 100 U/ml penicillin–streptomycin] in agar precoated flasks for 7–10 days. Enhanced GFP expressing NOD/SCID mice (Niclou *et al.*, 2008) were anaesthetized with a mixture of ketamine (10 mg/ml) and xylazine (1 mg/ml) and fixed in a stereotactic frame (Narishige Group). Tumour spheroids with a diameter of 200–300 μm (5–6 spheroids/mouse) were implanted into the right frontal cortex using a Hamilton syringe. Tumour take was ∼100% and time to sacrifice varied between 1 and 5 months depending on the original biopsy (Supplementary Table 1). In contrast with classical adherent glioblastoma cultures and glioblastoma stem-like cells known to lose typical glioblastoma characteristics such as for example, amplification and expression of EGFR (Huszthy *et al.*, 2012; Schulte *et al.*, 2012), the organotypic spheroid-based xenografts closely maintain the phenotypic and genetic profile of the original patient tumours (Sakariassen *et al.*, 2006; De Witt Hamer *et al.*, 2008; Wang *et al.*, 2009). Animals were sacrificed at the appearance of neurological symptoms and weight loss. For cancer stem cell lines 5×10^5 cells were injected in a 2 μl volume. Temozolomide treated animals (T16 xenografts, $n = 5$) received intraperitoneal injections of temozolomide (Sigma 200 mg/kg in 10% dimethyl sulphoxide) three times a week, starting 2 weeks after spheroid implantation. For anti-angiogenic treatment, animals (P3 xenografts, $n = 5$) received weekly intraperitoneal injections of bevacizumab (Avastin, Roche; 20 mg/kg in saline), starting 3 weeks after spheroid implantation. Control animals received injections of 10% dimethyl sulphoxide or saline. All procedures were approved by the national authorities responsible for animal experiments in Luxembourg.

Cell culture

The glioblastoma stem-like lines NCH644 and NCH421k, kindly provided by Dr Christel Herold-Mende (Department of Neurosurgery, University of Heidelberg) (Campos *et al.*, 2010), were cultured as non-adherent spheres in Neurobasal® medium (Invitrogen) containing $1 \times$ B27 (Invitrogen), 2 mM L-glutamine, 30 U/ml penicillin–streptomycin, 1 U/ml heparin (Sigma), 20 ng/ml bFGF (Miltenyi, 130-093-841) and 20 ng/ml EGF (Provitro, 1325950500) (neural stem cell medium).

Side population assay combined with multicolour cell membrane phenotyping

Glioblastoma tumour biopsies, xenografts and control mouse brains were minced with scalpels and dissociated with MACS® Neural Tissue Dissociation Kit (P) (Miltenyi, 130-092-628) following the manufacturer's instructions. Cultured cell lines were trypsinized (0.25% trypsin; Lonza) at 37°C for 2–3 min. Single cell suspensions were resuspended in prewarmed Dulbecco's modified Eagle medium, containing 2% foetal bovine serum, 10 mM HEPES pH 7.4 and DNase I (10 μg/ml; Sigma) at 1×10^6 cells/ml followed by preincubation with or without ABC transporter inhibitors: verapamil (250 μM; Sigma) and fumitremorgin C (FTC, 10 μM; Calbiochem) for 20 min at 37°C, and a 90–120 min incubation with Hoechst 33342 (5 μg/ml, bisbenzimide, Ho342; Sigma) at 37°C with gentle agitation on a shaker.

After washing, cells were resuspended in ice-cold Hank's balanced salt solution, 2% foetal bovine serum, 10 mM HEPES pH 7.4 buffer (100 μl/test). Prior to flow cytometry, cells were incubated with LIVE/DEAD® Fixable Dead Cell Stains (Invitrogen; 1 μg/ml) and appropriate preconjugated antibodies for 30 min at 4°C in the dark (antibodies are listed in Supplementary Table 3). Data acquisition was performed on a fluorescence-activated cell sorting Aria™ SORP cytometer (BD Biosciences) and the Hoechst signal was excited with the UV laser (Supplementary material). Data acquisition and analysis were done with DIVA software (BD Bioscience). Histograms were prepared with the FlowJo software. For sorting experiments, cells were collected in ice-cold Hank's balanced salt solution containing 10% foetal bovine serum, 10 mM HEPES pH 7.4 buffer and cultured at varying concentrations (10 000–100 000 cells/well in a 24 well plate) in (i) tumour conditions: spheroid medium in agar pre-coated plates; (ii) endothelial cells conditions: endothelial basal medium-2 supplemented with EGM®-2 BulletKit® (all from LONZA, CC-3124) on fibronectin precoated surface; and (iii) neural stem cell conditions: neural stem cell medium without coating.

Fluorescence *in situ* hybridization

Sorted cells isolated from primary glioblastomas were cytospinned for 15 min, 1000 rpm onto glass coverslips. Cells were treated with 0.4% KCl, fixed in methanol/glacial acetic acid solution (3:1), dehydrated in a series of 70%, 90% and 100% ethanol (3 min each) and dried at 37°C. Fluorescence *in situ* hybridization probes were designed to include gained or lost regions based on array comparative genomic hybridization results (Supplementary Table 1). Bacterial artificial chromosomes, provided by the Deutsches Ressourcenzentrum für Genomforschung (Berlin, Germany), were labelled using nick-translation (Klink *et al.*, 2010). The probe set used for T330 and T341: RP1189e8 + RP11815k24 on 7p12 [including *EGFR*; Atto 488-dUTP-NT (Jena Bioscience); 'green'], RP11-165m8 on 10q23.3 [including *PTEN*; tetramethyl-rhodamin-5-dUTP (Roche); 'red'], RP11-427a8 + RP11-1012c18 on 7q31 [including *MET*; aqua-5-dUTP (Enzo Life Science), 'blue']. The probe set for T316: RP11-165m8 on 10q23.3 (as above) and two commercial probes targeting centromere 3 (Kreatech; 'green') and telomere 18q (Kreatech; 'blue'). Fluorescence *in situ* hybridization was carried out according to standard protocols. Fluorescence *in situ* hybridization probe sets were validated on unsorted patient tumour cells and lymphocytes of normal control individuals.

Gene expression analysis

Total RNA was extracted using a standard TRIzol® extraction protocol. One microgram of total RNA was reverse transcribed using iScript™ cDNA synthesis Kit (Biorad) according to the manufacturer's instructions and real-time quantitative PCR was carried out using Fast SYBR® Green Master Mix and the Viia™ 7 Real Time System (Applied Biosystems). See Supplementary Table 4 for oligonucleotides used. Amplification temperature was kept at 60°C. Cycle threshold (Ct) values were determined in the exponential phase of the amplification curve and the $\Delta \Delta CT$ method was used for fold change calculations (QBase software). All samples were run in triplicates and the data was analysed with unpaired independent-samples *t*-test (Excel software). Statistical significance was set for two levels *$P < 0.05$ and **$P < 0.005$.

Results

Glioblastoma patient biopsies contain non-neoplastic, stroma-derived side population cells

Since cancer stem-like cells are characterized by increased resistance to chemotherapy, we wanted to address the question to what extent increased side population efflux properties are linked to glioblastoma stem-like cells. We applied the flow cytometric side population discrimination assay on fresh glioblastoma patient tumour samples obtained directly after surgery to visualize side population cells as a dim tail of events with decreased fluorescence in two Hoechst channels (Golebiewska *et al.*, 2011). Eight different patient samples were analysed (Supplementary Table 1). Following a rigorous side population assay protocol and an appropriate gating strategy (Supplementary Fig. 1) to analyse single viable nucleated cells, we detected a visible side population in all glioblastoma biopsies ranging from 0.1–11.2% of the total cell number analysed (Fig. 1A, additional examples are shown in Supplementary Fig. 2). The side population phenotype was confirmed by appropriate inhibition controls (Supplementary Fig. 2). To determine the nature of side population cells, side population and non-side population cells (main population) were sorted from fresh patient biopsies and analysed at the single cell level by fluorescence *in situ* hybridization. Fluorescence *in situ* hybridization probes were designed to distinguish between normal and tumour cells and adapted to the genomic profile of each biopsy as determined by array comparative genomic hybridization (Supplementary Table 1). We found that all side population cells from patient samples showed two signals for each fluorescence *in situ* hybridization probe, characterizing them as normal stromal cells (Fig. 1B). In contrast, the main population cells always consisted of a mixture of normal and tumour cells (17–43% tumour cells depending on the biopsy), with patient-specific aberrations such as amplification of the epithelial growth factor receptor (*EGFR*) gene and loss of chromosome 10 (Fig. 1B).

Since sorting of patient biopsies yielded insufficient material for subsequent analysis (<1500 cells per patient biopsy), we established intracranial xenografts in enhanced green fluorescent protein (GFP) expressing NOD/SCID mice from spheroids derived from four glioblastoma patient biopsies. We have previously shown that such biopsy-derived xenografts fully maintain the genetic and phenotypic characteristics of patient tumours including diffuse infiltration into the brain parenchyma and angiogenesis (Wang *et al.*, 2009; Keunen *et al.*, 2011; Huszthy *et al.*, 2012). The implantation into enhanced GFP expressing mice enabled a clear fluorescence-based discrimination of implanted tumour cells from enhanced GFP-positive host cells both on tissue sections and by fluorescence-activated cell sorting analysis (Fig. 1C). This was crucial because normal healthy brain contains side population cells, as shown in Fig. 1D. All mice implanted with glioblastoma spheroids generated tumours. Importantly, in all xenografts, similar to fresh patient biopsies, flow cytometric analysis revealed the presence of side population cells (Fig. 1E, additional examples are

shown in Supplementary Fig. 3). However, upon fluorescence-based discrimination between the tumour and stromal compartment, all side population events turned out to be enhanced GFP-positive, clearly identifying them as host cells (Fig. 1E and Supplementary Fig. 3). We have previously shown that for complete inhibition of brain-derived side population two different ABC transporter inhibitors are required: verapamil for ABCB1 inhibition and fumitremorgin C for ABCG2 inhibition (Golebiewska *et al.*, 2011). As in patient biopsies, complete blockade of efflux properties in the xenografts also required the combination of both inhibitors (Fig. 1E and Supplementary Fig. 3). In summary, these results demonstrate that side population cells present within human glioblastoma belong to the non-neoplastic stromal compartment.

The glioblastoma side population phenotype is non-tumorigenic and this is independent of tumour genotype, phenotype or treatment

To further confirm the absence of tumour cells within the side population compartment, we determined the tumorigenic potential of side population and non-side population cells in glioblastoma xenografts. Side population cells ('stromal side population' cells) were separated by fluorescence-activated cell sorting from the main population of stromal cells ('stromal main population' cells) as well as from the main population tumour cells ('tumour main population' cells) (see Supplementary Fig. 4A–C for gating and quality control of sorted cells). As expected, side population cells were not able to form spheroids *in vitro* or grow tumours *in vivo* and only the tumour main population cells showed tumorigenic potential (Fig. 2A and B).

To verify that the lack of a side population group in tumour cells was not related to the genetic profile of human glioblastomas, five additional genetically divergent human glioblastoma cells were implanted into the brain of enhanced GFP NOD/SCID mice (see Supplementary Table 1 for overview of glioblastoma and array comparative genomic hybridization profiles). Similar to the previous xenografts, all xenografts displayed a side population, which upon tumour–host discrimination were found to be entirely host-derived independent of the chromosomal aberrations within the tumour (Fig. 2C and Supplementary Fig. 5A). Because the ploidy of tumour cells varies between patients and influences the identification of side population cells, an example of an aneuploid (T101) and a diploid glioblastoma (T185) is depicted in Fig. 2C (with additional examples in Supplementary Fig. 5A). The ploidy of the tumour cells was assessed by comparison to the Hoechst level of diploid mouse cells. In all cases the tumour cells could be adequately separated from enhanced GFP-positive host cells and were never found in the side population fraction.

To characterize the side population phenotype in relation to cancer stem cell associated marker expression in patients with glioblastoma, we determined the expression level of CD133 and CD15 in the tumour populations. Interestingly, the tumours contained a highly variable percentage and a variable expression level of CD133$^+$ and CD15$^+$ tumour cells (Supplementary Fig. 5B). Therefore we conclude that the identification of stromal-derived
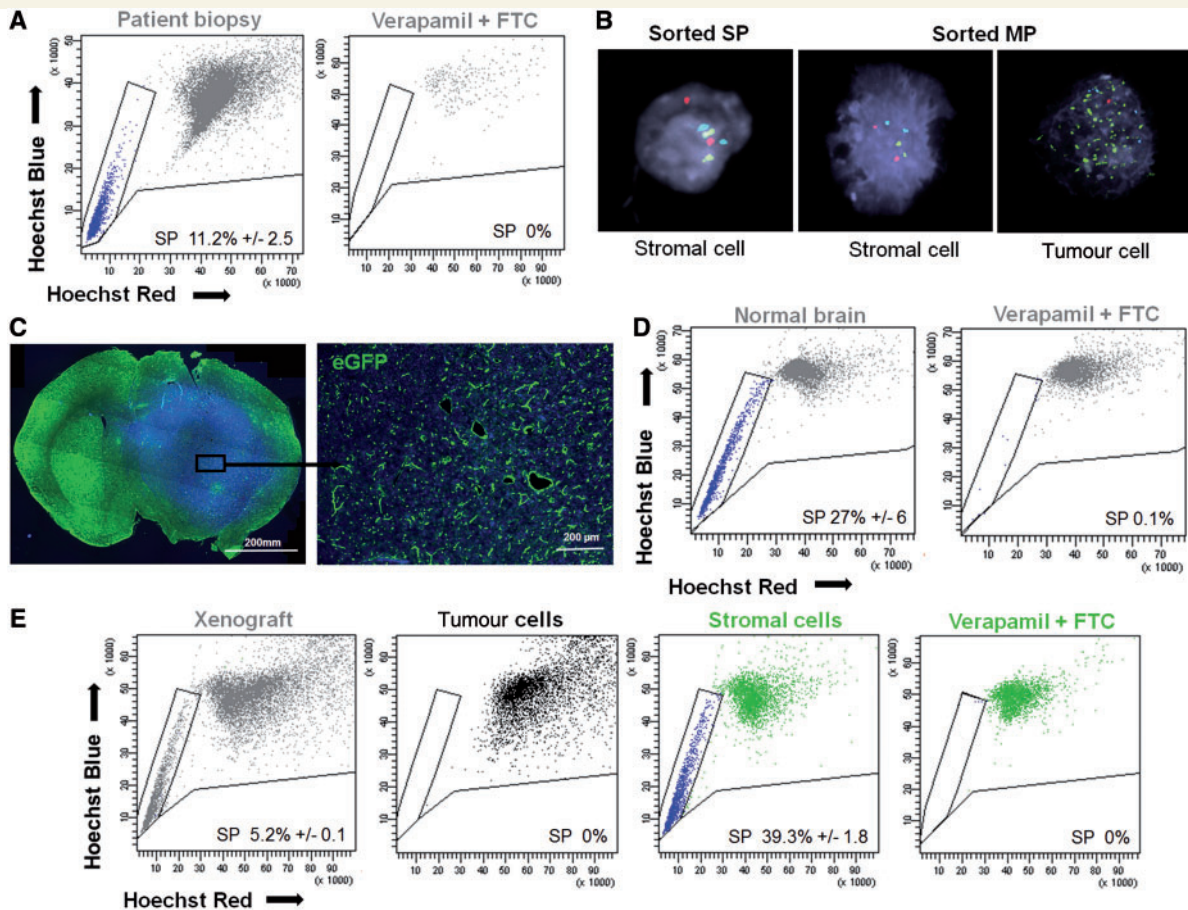
Figure 1 The side population in glioblastoma patient biopsies is non-neoplastic. (**A**) Side population (SP) discrimination assay performed on human glioblastoma: viable, single and nucleated cells (grey) of tumour biopsies (shown for T316) contained a visible side population (blue) identified as a well-defined characteristic 'tail' with a decreased Hoechst signal in both 'Hoechst' channels. Dye efflux was confirmed by double inhibition with 250 μM verapamil and 10 μM fumitremorgin C (FTC). Additional examples in Supplementary Fig. 2. (**B**) Fluorescence *in situ* hybridization analysis of side population and main population (MP) cells sorted from patient biopsies demonstrates the lack of tumour cells in the side population fraction (example shown for T330). Tumour cells showed typical glioblastoma aberrations [red probe = 10q23 (PTEN) deletion, green probe = EGFR amplification, blue probe = 7q trisomy]. (**C**) Glioblastoma spheroid-derived xenograft developed in the brain of enhanced GFP expressing NOD/SCID mice was recognized as a region with increased cellularity (DAPI = blue) and decreased enhanced GFP signal (green) (*left*). Higher magnification of the boxed area showing the presence of green host cells within the non-green human tumour tissue (*right*). (**D**) Normal mouse brain contained the side population phenotype (*left*), as confirmed by the inhibition control (250 μM verapamil + 10 μM fumitremorgin C) (*right*) (*n* = 8). (**E**) Side population phenotype was also detected in viable, single and nucleated cells of the patient-derived xenografts (T238) in enhanced GFP[+] NOD/SCID mice (grey) (*n* = 3). Discrimination between host stromal (green) and tumour (black) compartment revealed side population uniquely in the stromal compartment of the xenograft (blue). Data are presented as a mean value ± SEM, *n* ⩾ 4. For patient biopsies SEM represents technical replicates. See Supplementary Fig. 1 for detailed gating strategy and Supplementary Fig. 3 for additional examples of xenografts.

glioblastoma side population cells appears to be independent of cancer stem-like cell marker expression in tumour cells. We also addressed the question whether side population phenotype induction might occur by cytotoxic drugs, as has earlier been suggested in a transgenic glioma model (Bleau *et al.*, 2009). Human glioblastoma xenografts treated with the alkylating agent temozolomide, the standard chemotherapy for patients with glioblastoma, retained the same Hoechst profile as untreated tumours both in the tumour and the stromal compartments (Supplementary Fig. 5C). Taken together, our findings indicate that in human glioblastoma the side population phenotype is non-tumorigenic and is limited to the stromal compartment. Lack of efflux properties in

tumour cells is independent of the ploidy, the genetic profile of the tumour, and cancer stem-like cells associated marker expression in the tumour, thus excluding the side population phenotype as a marker for glioblastoma stem-like cells.

The side population phenotype is absent in glioblastoma stem-like cells *in vitro* and *in vivo*

We also assessed the side population phenotype in glioblastoma stem-like cell lines which express high levels of CD133 and CD15
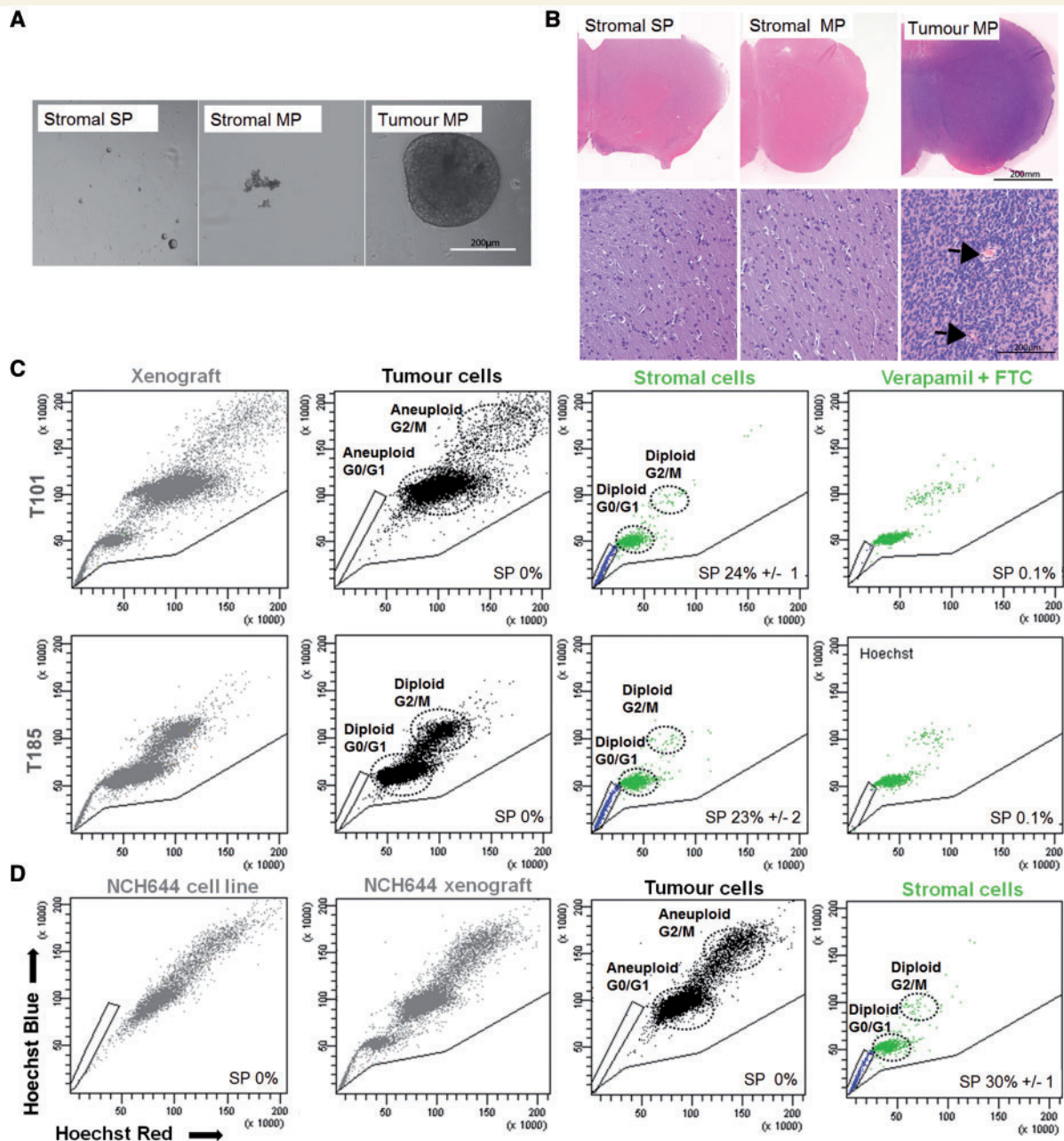
Figure 2 The side population in human glioblastoma xenografts is exclusively present in the non-tumorigenic stromal compartment. (**A**) Stromal side population, stromal main population and tumour main population cells isolated from T16 xenografts by fluorescence-activated cell sorting were cultured in spheroid medium under non-adherent conditions (equal cell numbers, 10–100 000 cells/well; *n* = 4) *in vitro*. Only cells from the tumour main population formed spheroids within 2 weeks of culture. To increase the number of events and the purity of the gates used for sorting, human-specific EGFR staining was added to enhanced GFP discrimination. See Supplementary Fig. 4A for gating strategy, sorting controls and xenograft analysis. (**B**) Sorted cells from T16 xenograft were implanted intracranially into NOD/SCID mice (50 000 cells/animal; *n* = 5). At 10 weeks the tumour main population group had developed large tumours that displayed characteristic glioblastoma features, including invasion to contralateral hemisphere and aberrant blood vessels (arrows), while no tumours were seen with the stromal side population or stromal main population groups even after 20 weeks. (**C**) Glioblastoma xenografts derived from different patient biopsies (T101 and T185) displayed a heterogeneous Hoechst profile (grey). Tumour cells displayed varying ploidy (T101 aneuploid; T185 diploid) and side population gates were adjusted accordingly. However after tumour/host discrimination, all side population events appeared to be uniquely stroma-derived (blue). Dye efflux was confirmed by inhibition controls (250 μM verapamil + 10 μM fumitremorgin C). Additional examples are shown in Supplementary Fig. 5A. (**D**) NCH644 glioblastoma cells cultured under stem cell conditions *in vitro* was devoid of side population (*n* = 5) (*left*). In NCH644 xenografts the Hoechst profile on viable, single and nucleated cells (grey) was heterogeneous. After tumour/host discrimination side population events (blue) appeared to be uniquely stroma-derived. Side population gates were adjusted according to cell ploidy, where NCH644 cells appeared aneuploid (*n* = 4). MP = main population; SP = side population.

(Supplementary Fig. 5D). In analogy to classical adherent glioblastoma cell lines shown to be side population-negative (Golebiewska *et al.*, 2011) and in agreement with previous reports (Broadley *et al.*, 2011), we did not detect side population cells in the stem-like lines (NCH644 and NCH421k) grown as sphere cultures under serum-free conditions (Fig. 2D and Supplementary Fig. 5E). This outcome was also not affected by hypoxic culture conditions (0.1–1% O_2) (not shown). Since long term cultures lead to a reduction of dye efflux properties (Torok *et al.*, 2003), we analysed the side population profile of stem-like cells *in vivo* as intracranial xenografts. Similar to spheroid-based xenografts, the side population of glioblastoma stem-like cell line derived xenografts was detected only within the enhanced GFP-positive stromal compartment (Fig. 2D and Supplementary Fig. 5E).

The side population phenotype in glioblastoma biopsies is strongly enriched in endothelial cells

Glioblastomas recruit different types of non-neoplastic cells including endothelial cells, hematopoietic cells, mesenchymal and neural stem cells, which could represent a potential source of the side population (Aboody *et al.*, 2000; Bjerkvig *et al.*, 2009; Klopp *et al.*, 2011). One of the difficulties in identifying cells in the brain is the lack of cell-type-specific markers, which are often shared by several cell types e.g. nestin is expressed by neural stem cells, neural progenitors as well as endothelial cells (Najbauer *et al.*, 2012). Moreover, in brain neoplasms these markers can also be expressed by subpopulations of tumour cells. We therefore combined the side population phenotype assay with multicolour cell membrane phenotyping to determine the cellular identity of side population cells in fresh glioblastoma patient biopsies (see Supplementary Table 2 for markers used in this study).

To discriminate between tumour and stromal cells, tumour cells were identified by *EGFR* expression (Fig. 3A), which is present in the majority of glioblastomas and can be detected by highly sensitive flow cytometric analysis even in the absence of *EGFR* gene amplification (not shown). As expected, side population cells were exclusively found in the EGFR-negative fraction. The vast majority of side population cells stained positive for the endothelial cell marker CD31 (Fig. 3A), with co-expression of CD105 (Supplementary Fig. 6A), indicating that in glioblastoma patient biopsies, side population cells are largely composed of endothelial cells. This was confirmed in side population cells from five representative human glioblastomas (Fig. 3B and C). We further examined the presence of the side population phenotype in cell populations expressing glioblastoma cancer stem-like cell associated markers. Although efflux properties were present within CD133^{+} and A2B5^{+} cells (Fig. 3D) these were all EGFR-negative (e.g. Supplementary Fig. 6B). In fact all CD133^{+} cells within the side population co-expressed CD31 confirming their endothelial identity, while CD133^{+}CD31^{-} cells were never associated with the side population (Fig. 3E). None of the other subpopulations, including CD15^{+} and CD44^{+} cells (Fig. 3F) as well as hematopoietic CD45^{+} cells (Supplementary Fig. 6C) showed side population characteristics. In conclusion, our data show that the side population phenotype in human glioblastoma is restricted to CD31^{+}CD133^{+} endothelial cells and A2B5^{+} stromal cells. These results highlight the importance of multicolor phenotyping to discriminate cell populations in complex tumour tissue, since many markers including glioblastoma stem-like cell markers are expressed both in tumour and stromal cells.

The side population in glioblastoma xenografts and normal brain contains endothelial cells and astrocytes, but is absent from adult neural stem/progenitor cells

To further confirm the cellular identity of side population cells we performed detailed multicolour phenotyping of stromal cells in glioblastoma xenografts generated in enhanced GFP expressing mice. The vast majority of side population cells in the xenografts (87–96%) stained positive for the mouse-specific endothelial cell markers CD31, CD133, CD105 and CD90 (Fig. 4A, B, Supplementary Fig. 7A and B), thus confirming their endothelial cellular identity. Similarly, side population cells in normal brain were almost exclusively composed of endothelial cells (Fig. 4B). Because CD105 and CD90 are expressed by different cell types in the brain, it is important to note that CD105^{+} and CD90^{+} side population cells invariably co-expressed CD31 and CD133 confirming their endothelial identity (not shown). In addition to endothelial cells, the side population contained a small proportion of A2B5^{+}CD44^{low} astrocytic cells both in xenografts and normal brain (3–7% of the side population) (Fig. 4B). These cells might represent perivascular astrocytes known to express ABC transporters in their end-feet surrounding blood vessels (Golden and Pardridge, 1999) (Supplementary Fig. 7D).

To identify neural stem/progenitor cells in xenografts and in normal brain, we applied CD133 and CD15 marker expression combined with CD31 and CD44 negativity. A small percentage of CD31^{-}CD133^{+} cells (<0.4%, Fig. 4A) which were also CD44^{-} (not shown), representing putative neural stem/progenitor cells, were observed in the main population, but not in the side population of either xenograft or normal brain. Co-staining of CD133 with CD15 revealed CD15^{+}CD133[+/-]CD31^{-}CD44^{-} cells, which were never found in the side population (Fig. 4B and Supplementary Fig. 7C). These data indicate that neural stem/progenitor cells in the adult brain do not display efflux properties, in contrast with their foetal counterpart. Of interest, the number of neural stem/progenitor cells strongly increased in the xenograft stromal compartment compared with the normal brain (3.3% versus 1.1%). The same was true for CD44^{+} cells, representing glial, mesenchymal and hematopoietic cells (Fig. 4B). These included CD11c^{+} microglia and macrophages, NG2^{+} activated pericytes and oligodendrocyte-like cells as well as low levels of putative CD105^{+}CD90^{+} mesenchymal stem cells (Fig. 4B, Supplementary Fig. 7A and B). Except for some CD11c^{+}CD44^{+} cells (<0.16% side population), all identified populations were exclusively in the non-side population (main population).
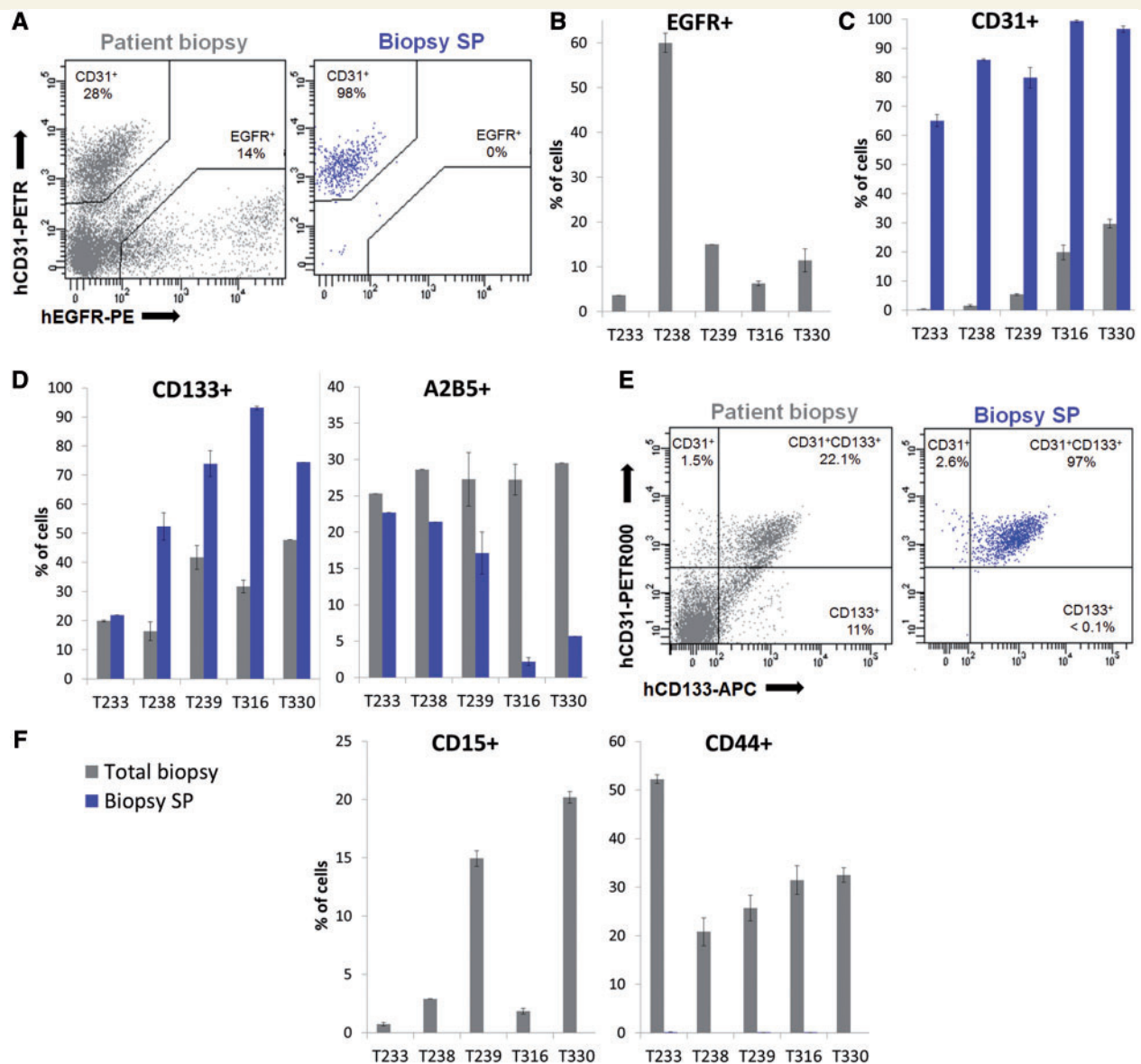
Figure 3 The side population in glioblastoma patient biopsies is enriched in stromal endothelial cells. (**A**) EGFR/CD31 phenotyping in patient biopsies revealed the presence of heterogeneous cell populations (total biopsy: grey). The vast majority of side population events (biopsy side population: blue) were CD31$^+$ and none were EGFR$^+$ (example shown for T330). (**B**) Although glioblastoma patient biopsies contained varying levels of tumour cells (shown here as EGFR$^+$) in each case the side population was devoid of EGFR$^+$ events (blue not detectable here). (**C**) The side population in each patient biopsy was strongly enriched in CD31$^+$ cells. (**D**) CD133$^+$ and A2B5$^+$ cells were present in total biopsy, and were also detected in the side population fraction of patient biopsies. (**E**) Of note all CD133$^+$ side population cells co-expressed CD31 (shown for T316). (**F**) The side population did not contain CD15$^+$ and CD44$^+$ cells ($n = 3$). For patient biopsies error bars represent technical replicates. Total biopsy = grey; biopsy side population = blue. MP = main population; SP = side population.

The flow cytometric phenotyping was corroborated by quantitative PCR analysis for lineage-specific intracellular markers. A strong enrichment of von Willebrand Factor (*vWF*) (Fig. 4C), nestin and vimentin (Supplementary Fig. 7E) in stromal and brain side population further confirmed the endothelial cell nature of these cells. Glial fibrillary acidic protein (*GFAP*), an astrocytic marker, was detected at a low level in stromal and brain side population (0.3 to 0.5-fold change, Fig. 4C). The microglia marker *AIF1*, the oligodendrocyte marker *OLIG2* and the pericyte/mesenchymal stem cell marker desmin were present almost exclusively in

the stromal main population and brain main population (Fig. 4C). In a functional assay only cells from stromal side population (Fig. 4D) and brain side population (not shown) were able to survive in endothelial cell medium, while in neural stem cell medium, neurospheres were generated exclusively from the stromal main population (Fig. 4E) and brain main population (not shown), but not from side population cells.

Taken together, we show that the side population of the stromal compartment in glioblastoma xenografts, contains exclusively endothelial cells and A2B5$^+$ astrocytes, in agreement with the
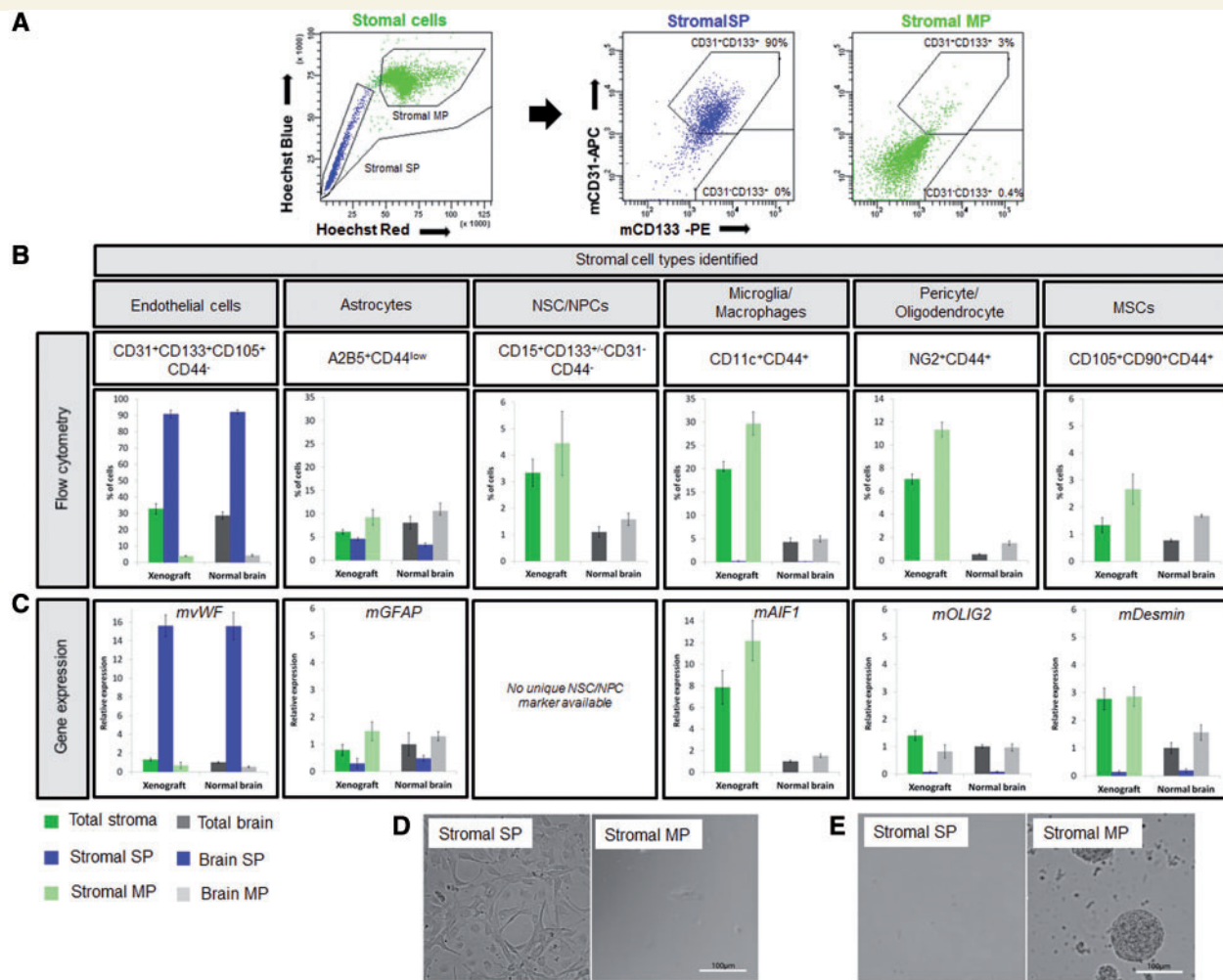
Figure 4 Stromal cells with functional efflux properties within glioblastoma xenografts belong to endothelial and astrocytic populations. (**A**) Side population analysis (*left*) and CD133/CD31 phenotyping in the stromal compartment of the T16 xenograft (*right*). More than 90% of the stromal side population (blue) was CD31$^+$CD133$^+$, whereas CD31$^-$CD133$^+$ cells were devoid of a side population. Stromal main population (light green) contained 0.4% of CD31$^-$CD133$^+$ and only 3% of CD31$^+$CD133$^+$ events. (**B**) For identification of stromal cells, side population analysis was combined with multicolour phenotyping using antibodies against mouse epitopes and results were compared to normal mouse brain. Percentages of subpopulations of cells detected in the stromal compartment of the xenograft and normal brain were calculated for the whole single nucleated viable population (total stroma and total brain), side population (stromal side population and brain side population) and main population cells (stromal main population and brain main population) ($n \geqslant 4$). See Supplementary Table 2 for cell membrane marker expression profile. Side population events were identified as CD31$^+$CD133$^+$CD105$^+$CD44$^-$ endothelial cells (first panel) and A2B5$^+$CD44^{low} astrocytic cells (second panel). Other populations characterized did not contain side populations (panels 3–6). Note that the A2B5$^+$ side population cells co-expressed the glial marker CD44 at a medium/low level and were therefore not included in the CD44$^+$ populations in our calculations. (**C**) Expression of lineage-specific markers was analysed by quantitative real-time-PCR. Mouse-specific actin and *GAPDH* were used as reference genes. The data are presented as mean ± SEM ($n = 3$). Normal brain (total brain) was used as an internal calibration (value = 1). See Supplementary Table 2 for internal cell marker expression profile and Supplementary Fig. 4 for sorting controls. Unfortunately none of the neural stem/progenitor cell markers was specific enough for PCR analysis, since nestin, vimentin (Supplementary Fig. 7E), *SOX2* and *GFAP* are also expressed by other cell types in the brain. Desmin was used as a marker of pericytes and mesenchymal stem cells. (**D**) When sorted stromal side population and stromal main population cells were cultured in endothelial cell medium, only cells from the side population fraction were able to survive under these conditions. Only at high cell concentrations (100 000/well) occasional endothelial cells present within the main population survived. (**E**) Under neural stem cell conditions neurospheres developed only from the main population fraction (10 000 cells/well). MP = main population; MSC = mesenchymal stem cells; NPC = neural precursor cell; NSC = neural stem cell; SP = side population.

data obtained in fresh patient biopsies. This was also true for the side population of the normal adult brain and is in accordance with previous reports, where the side population phenotype has been associated with endothelial/hematopoietic-like cells in the normal brain (Mouthon *et al.*, 2006). Other stromal cells attracted to the tumour, such as stem/progenitor cells of neural or mesenchymal origin as well as microglia, macrophages and pericytes lack efflux properties.

Functional efflux properties in glioblastoma stromal cells rely on ABCB1, ABCG2 and ABCC4 transporters

To unravel the molecular basis of the efflux properties in glioblastoma-derived side populations we performed gene expression analysis for ABC transporters in the stromal compartment of the xenografts (stromal side population and stromal main population) and normal brain (brain side population and brain main population). *ABCB1A*, *ABCG*2 and *ABCC4* were highly enriched in stromal and brain side population (Fig. 5A). Importantly, the level of expression between stromal and brain side populations was very similar, confirming similar efflux properties in these two populations. Other transporters were hardly expressed in the side population (*ABCC1*, *ABCC5* Supplementary Fig. 7F) or were found at a higher level in the main populations (e.g. *ABCB1B* Fig. 5A; *ABCC2*, *ABCC3* Supplementary Fig. 7F), indicating that they are not involved in efflux properties in the brain. The expression of ABCB1 and ABCG2 proteins was confirmed by cell membrane staining, where side population in glioblastoma patient biopsies was double positive for both ABC transporters (Fig. 5B). Similar to normal brain, CD31$^+$CD133$^+$ endothelial cells from patient biopsies and xenografts appeared mostly as a 'low side population' (Fig. 5C). Also in analogy to the normal brain, blocking the efflux potential of endothelial cells within the tumour tissue required the combination of the two inhibitors verapamil and fumitremorgin C at high concentration (Fig. 5C). In summary, our data show that efflux properties of the normal brain vasculature are preserved in tumour vessels and rely on the functional ABC transporters, ABCB1 and ABCG2.

The efflux properties of stromal endothelial cells are retained after anti-angiogenic treatment

There is currently a considerable debate about whether vessel normalization in brain tumours as observed upon treatment with anti-angiogenic agents will enhance or impair the delivery of concomitant chemotherapeutic drugs (Batchelor *et al.*, 2007; Claes *et al.*, 2008). Although several studies have addressed the restoration of the blood–brain barrier at the macroscopic level using non-invasive imaging techniques, no data are currently available on the functional properties of endothelial cells in response to anti-angiogenic treatment. We therefore addressed whether the efflux properties of brain endothelial cells were affected after treatment with bevacizumab, a blocking antibody against vascular endothelial growth factor (VEGF). For this purpose we used an angiogenic glioblastoma xenograft (Keunen *et al.*, 2011) that displays a high percentage of side population cells (Supplementary Fig. 4A), thus indicating a large number of endothelial cells within the host cellular compartment. As shown previously, bevacizumab treatment did not increase survival (Fig. 6A); despite the fact that blood vessel density was decreased within the tumours (Fig. 6B). Flow cytometric analysis confirmed that the percentages of total

side population as well as endothelial cells (CD31$^+$CD133$^+$CD44$^-$) were significantly decreased after bevacizumab treatment (Fig. 6C). Nevertheless, the remaining endothelial cells present in treated xenografts displayed strong efflux properties, as shown by their appearance as a low side population, equivalent to the untreated controls (Fig. 6D). Taken together these data indicate that endothelial cells in glioblastomas remain metabolically active and possess undiminished efflux properties after anti-angiogenic treatment.

Discussion

The heterogeneity of tumour tissue, the lack of specific markers and their relative scarcity pose serious challenges to the identification of glioblastoma stem-like cells. Because of their proposed chemoresistance, we applied a detailed side population discrimination assay to identify stem-like cells in human glioblastomas. Here we show that efflux properties based on ABC transporters are absent in human glioblastoma cells, indicating that the side population phenotype cannot be used to define glioblastoma stem-like cells. Moreover, side population properties were not induced by microenvironmental stress caused by hypoxia or cytotoxic drugs. The side population phenotype, which is present in human glioblastoma tissue, was entirely stroma-derived and could be identified as endothelial cells with a small contribution of astrocytes. Interestingly the efflux properties of endothelial cells were not affected by anti-angiogenic treatment.

To our knowledge this is the first study addressing the nature of side population cells in fresh tumour tissue of human glioblastoma. Our results are in agreement with a recent *in vitro* study on glioblastoma cells cultured under stem cell conditions that were found to be devoid of a side population (Broadley *et al.*, 2011), and resolve the controversy about the side population phenotype in human glioblastomas *in vivo* by clearly demonstrating that side population cells in glioblastoma are non-neoplastic and do not identify stem-like cells. In this context it is important to emphasize that the side population discrimination assay is a highly sensitive technique that requires a stringent protocol and gating strategy in order to avoid false positive results (Golebiewska *et al.*, 2011). A direct data comparison is only possible if similar side population protocols and gating strategies are applied. The violet laser used in earlier studies (Bleau *et al.*, 2009) was not sensitive enough for an adequate discrimination of the side population in normal brain and glioblastoma xenografts. Side population cells have been found in some neoplasms including breast cancer and have been described to possess higher clonogenic and tumorigenic potential, and increased resistance to chemotherapy as compared with non-side population cells (Wu and Alman, 2008). However, the majority of cancer cell lines and primary neoplasms including glioblastomas, appear to lack efflux properties, indicating that factors such as tumorigenicity, the stem-like phenotype and chemoresistance are not exclusively dependent on side population properties.

We further provide a detailed characterization of the stromal cells present within glioblastomas. By combining the side population assay with multicolour cell membrane phenotyping we were able to distinguish several stromal cell populations in patient
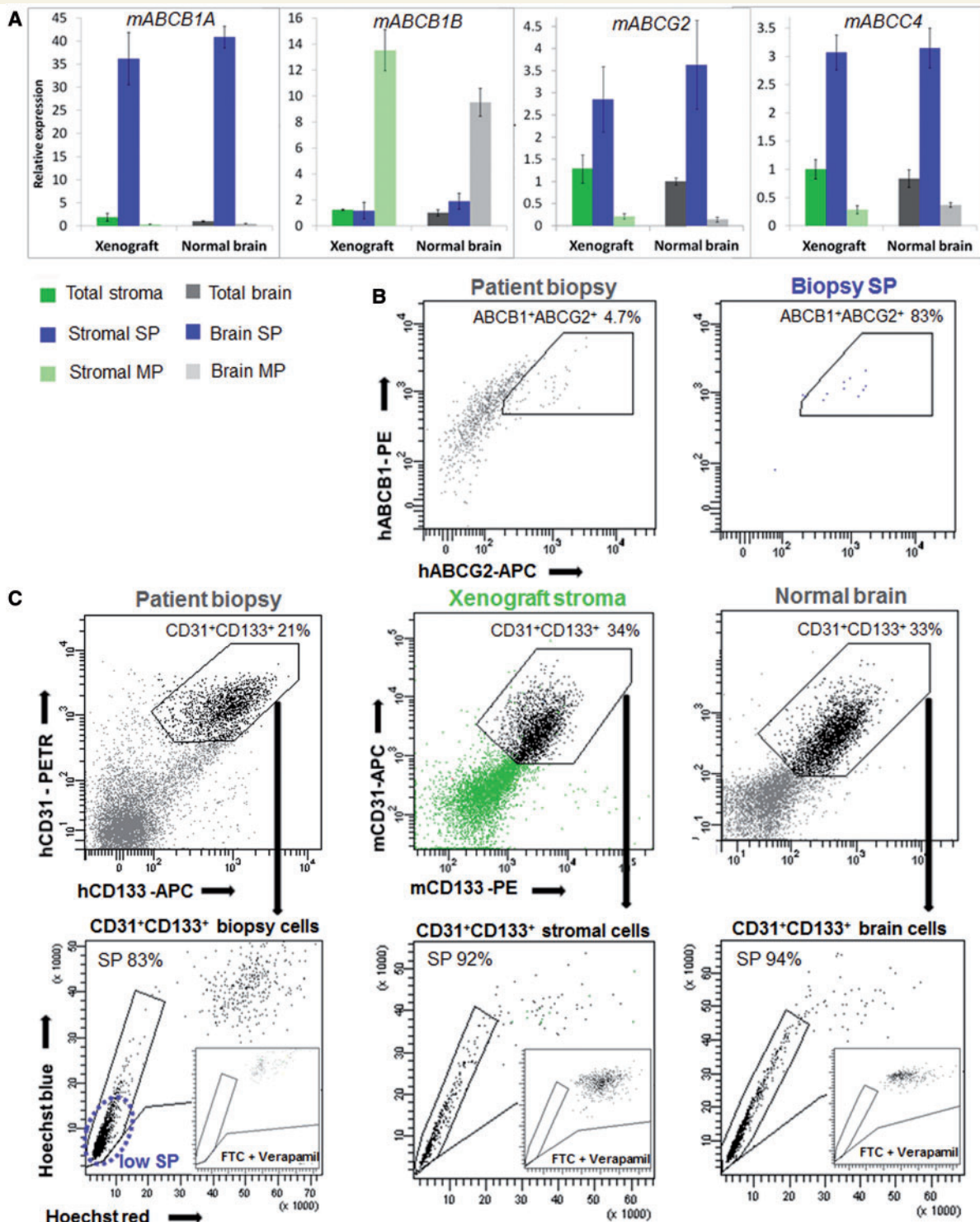
Figure 5 Efflux properties of brain endothelial cells are preserved in glioblastoma stroma. (**A**) Expression of ABC transporters was examined in sorted xenograft and normal brain side population and main population fractions using quantitative real-time-PCR. *ABCB1A*, *ABCG2* and *ABCC4* transporters were enriched in the side population, and their expression profile was comparable between the stromal compartment of xenograft and normal brain. Mouse-specific actin and *GAPDH* were used as reference genes. The data are presented as mean ± SEM (*n* = 3). Normal brain (total brain) was used as an internal calibrator (value = 1). See Supplementary Fig. 4 for sorting controls and Supplementary Fig. 7F for expression of other ABC transporters. (**B**) ABCB1/ABCG2 phenotyping of a glioblastoma patient biopsy revealed double positivity of biopsy side population cells for the two transporters (shown for T238). (**C**) Efflux properties of endothelial cells in patient biopsies, xenografts and normal brain. More than 80% of CD31^{+}CD133^{+} endothelial cells in the patient biopsy (shown for T316) and >90% of CD31^{+}CD133^{+} endothelial cells in glioblastoma xenografts (shown for T16) were in the side population, where most of the signal was detected at the tip of the 'side population tail' (low side population), similarly to normal brain endothelial cells. The combination of 10 μM fumitremorgin C and 250 μM verapamil was necessary for endothelial cell side population inhibition in all cases (insets). MP = main population; SP = side population.
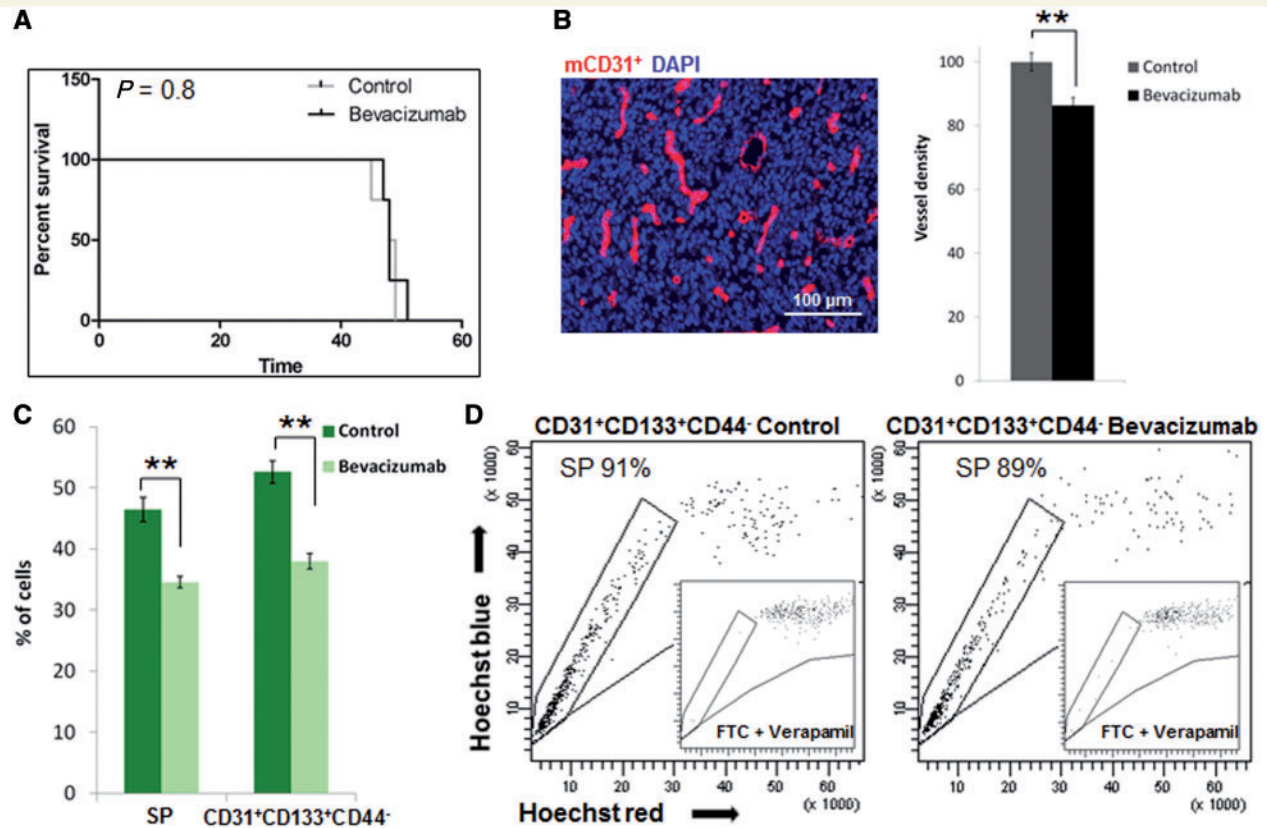
Figure 6 Side population properties of stromal endothelial cells are retained upon anti-angiogenic treatment. (**A**) Bevacizumab treatment in P3 xenografts did not prolong the survival of tumour-bearing mice (Kaplan–Meier plot). (**B**) Tumour vasculature was recognized by mouse-specific CD31 staining (*left* panel). Quantification of mCD31$^+$ blood vessels (red) indicated a reduction in the total vessel density after bevacizumab treatment in P3 xenografts; ($n = 5$) **$P < 0.005$ (t-test). (**C**) The percentage of side population and endothelial cells (CD31$^+$CD133$^+$CD44$^-$) detected in the stromal compartment of the xenograft was calculated for the GFP$^+$ single nucleated viable population in the control and bevacizumab treated P3 xenografts. A significant decrease in the number of side population and of endothelial cells was observed upon treatment. The data are presented as mean ± SEM ($n = 3$); **$P < 0.005$. (**D**) Efflux properties of endothelial cells were maintained after bevacizumab treatment. About 90% of endothelial cells (CD31$^+$CD133$^+$CD44$^-$) were in the side population fraction regardless of bevacizumab treatment, and most of the signal was detected as a 'low side population'. Inhibition controls with fumitremorgin C and verapamil are shown in the insets. SP = side population.

biopsies, which was further confirmed and expanded upon in human glioblastoma xenografts using enhanced GFP expressing mice. In addition to endothelial cells and astrocytes, these included neural stem/progenitor cells, mesenchymal stem cells, pericytes, and microglia/macrophages. The latter four populations strongly accumulated in the glioblastomas compared with the normal brain parenchyma. The side population phenotype was clearly restricted to stromal CD31$^+$CD133$^+$ endothelial cells and A2B5$^+$ astrocytes. In support of previous data on adult neural stem cells in normal brain (Mouthon *et al.*, 2006), we found that none of the stem/progenitor populations present within glioblastomas, e.g. neural stem cells and mesenchymal stem cells, displayed dye efflux properties. In this context it is interesting to speculate that in the adult brain, efflux properties may not be required in these cells due to an established blood–brain barrier. This may also explain the lack of side population in human glioblastoma cells, which grow in an efflux protected environment, as compared with other tumour types such as breast cancer. Importantly, we show that cancer

stem-like CD133$^+$ cells in patient biopsies are not a homogenous population and include CD31$^+$ endothelial cells carrying efflux properties. We therefore propose the use of a detailed multicolour phenotyping assay for an adequate analysis of cancer stem-like cell populations in the brain, since many markers, including CD133 and nestin, which are typically associated with neural stem cells and cancer stem-like cells, are also detected in other cell populations such as brain endothelial cells.

The efflux properties in glioblastoma and normal brain vessels were found to rely on the ABC transporters ABCB1, ABCG2 and ABCC4, in agreement with a previous report showing a role for ABCB1 in the blood–brain barrier, while ABCC1 is more prominent in the blood–CSF barrier (Gazzin *et al.*, 2008). Interestingly we also found that in glioblastoma patient biopsies and in xenografts derived thereof, efflux properties in tumour vessels are fully functional, suggesting that the vessel leakiness in the tumour core may be due to mechanical abnormalities rather than a loss of functional endothelial cell properties. These data are in contrast to results

from a transgenic mouse model, where the efflux properties of brain endothelial cells were reported to be impaired in glioma tissue (Bleau et al., 2009). This discrepancy might be explained by abnormal features of the stromal compartment in RCAS PDGF-B-driven glioma models which differ from human tumours.

In clinical and preclinical studies anti-angiogenic treatment of glioblastoma has been shown to normalize blood vessels and prevent leakage of contrast agents suggesting a restoration of the blood–brain barrier (Reardon et al., 2008; Carmeliet and Jain, 2011; Keunen et al., 2011). An unanswered question of major clinical interest is whether this will improve or impede drug delivery to the brain. Here we show that the efflux properties of endothelial cells are retained in glioblastoma multiformes following anti-angiogenic treatment, suggesting that drug penetration through the blood–brain barrier may still be hampered by a functional drug-effluxing endothelium. Efficient drug delivery is a major concern in glioblastoma treatment, in particular with regard to the highly invasive component of glioblastoma, which is largely shielded by an intact blood–brain barrier. Given the protective role of drug efflux transporters of endothelial cells in the brain, transiently modulating transporter function on endothelial cells may improve drug delivery to target invasive glioblastoma cells. Unfortunately, currently available inhibitors of ABC transporters have been rather unsuccessful due to their toxicity (Fletcher et al., 2010). Therefore more potent and specific transport inhibitors will be required for application in the brain.

In conclusion our findings contribute to an unbiased identification of cancer stem-like cells and stromal cells in brain neoplasms, and provide novel insight into the complex issue of drug delivery to the brain. Since efflux properties of endothelial cells are likely to compromise drug availability, transiently targeting ABC transporters may be a valuable therapeutic strategy to improve treatment effects in brain tumours.

Acknowledgements

Funding

Supplementary material

Supplementary material is available at Brain online.

References

Aboody KS, Brown A, Rainov NG, Bower KA, Liu S, Yang W, et al. Neural stem cells display extensive tropism for pathology in adult brain: evidence from intracranial gliomas. Proc Natl Acad Sci USA 2000; 97: 12846–51.

Agarwal S, Sane R, Oberoi R, Ohlfest JR, Elmquist WF. Delivery of molecularly targeted therapy to malignant glioma, a disease of the whole brain. Exp Rev Mol Med 2011; 13: e17.

Anido J, Saez-Borderias A, Gonzalez-Junca A, Rodon L, Folch G, et al. TGF-beta receptor inhibitors target the CD44(high)/Id1(high) Glioma-Initiating cell population in human glioblastoma. Cancer Cell 2010; 18: 655–68.

Barrett LE, Granot Z, Coker C, Iavarone A, Hambardzumyan D, Holland EC, et al. Self-renewal does not predict tumor growth potential in mouse models of high-grade glioma. Cancer Cell 2012; 21: 11–24.

Batchelor TT, Sorensen AG, di Tomaso E, Zhang WT, Duda DG, et al. AZD2171, a pan-VEGF receptor tyrosine kinase inhibitor, normalizes tumor vasculature and alleviates edema in glioblastoma patients. Cancer Cell 2007; 11: 83–95.

Beier D, Schulz JB, Beier CP. Chemoresistance of glioblastoma cancer stem cells–much more complex than expected. Mol Cancer 2011; 10: 128.

Bernacki J, Dobrowolska A, Nierwinska K, Malecki A. Physiology and pharmacological role of the blood-brain barrier. Pharmacol Rep 2008; 60: 600–22.

Bjerkvig R, Johansson M, Miletic H, Niclou SP. Cancer stem cells and angiogenesis. Semin Cancer Biol 2009; 19: 279–84.

Bleau AM, Hambardzumyan D, Ozawa T, Fomchenko EI, Huse JT, Brennan CW, et al. PTEN/PI3K/Akt pathway regulates the side population phenotype and ABCG2 activity in glioma tumor stem-like cells. Cell Stem Cell 2009; 4: 226–35.

Broadley KW, Hunn MK, Farrand KJ, Price KM, Grasso C, Miller RJ, et al. Side population is not necessary or sufficient for a cancer stem cell phenotype in glioblastoma multiforme. Stem Cells 2011; 29: 452–61.

Campos B, Wan F, Farhadi M, Ernst A, Zeppernick F, Tagscherer KE, et al. Differentiation therapy exerts antitumor effects on stem-like glioma cells. Clin Cancer Res 2010; 16: 2715–28.

Carmeliet P, Jain RK. Principles and mechanisms of vessel normalization for cancer and other angiogenic diseases. Nat Rev Drug Discov 2011; 10: 417–27.

Challen GA, Little MH. A side order of stem cells: the SP phenotype. Stem Cells 2006; 24: 3–12.

Claes A, Wesseling P, Jeuken J, Maass C, Heerschap A, Leenders WP. Antiangiogenic compounds interfere with chemotherapy of brain tumors due to vessel normalization. Mol Cancer Ther 2008; 7: 71–78.

Chen R, Nishimura MC, Bumbaca SM, Kharbanda S, Forrest WF, Kasman IM, et al. A hierarchy of self-renewing tumor-initiating cell types in glioblastoma. Cancer Cell 2010; 17: 362–75.

De Witt Hamer PC, Van Tilborg AA, Eijk PP, Sminia P, Troost D, Van Noorden CJ, et al. The genomic profile of human malignant glioma is altered early in primary cell culture and preserved in spheroids. Oncogene 2008; 27: 2091–6.

Fletcher JI, Haber M, Henderson MJ, Norris MD. ABC transporters in cancer: more than just drug efflux pumps. Nat Rev Cancer 2010; 10: 147–56.

Gazzin S, Strazielle N, Schmitt C, Fevre-Montange M, Ostrow JD, Tiribelli C, et al. Differential expression of the multidrug resistance-related proteins ABCb1 and ABCc1 between blood-brain interfaces. J Comp Neurol 2008; 510: 497–507.

Golden PL, Pardridge WM. P-Glycoprotein on astrocyte foot processes of unfixed isolated human brain capillaries. Brain Res 1999; 819: 143–6.

Golebiewska A, Brons NH, Bjerkvig R, Niclou SP. Critical appraisal of the side population assay in stem cell and cancer stem cell research. Cell Stem Cell 2011; 8: 136–47.

Goodell MA, Brose K, Paradis G, Conner AS, Mulligan RC. Isolation and functional properties of murine hematopoietic stem cells that are replicating *in vivo*. J Exp Med 1996; 183: 1797–806.

Hirschmann-Jax C, Foster AE, Wulf GG, Nuchtern JG, Jax TW, Gobel U, et al. A distinct "side population" of cells with high drug efflux capacity in human tumor cells. Proc Natl Acad Sci USA 2004; 101: 14228–33.

Huszthy PC, Daphu I, Niclou SP, Stieber D, Nigro JM, Sakariassen PO, et al. *In vivo* models of primary brain tumors: pitfalls and perspectives. Neurooncology 2012; 14: 979–93.

Keunen O, Johansson M, Oudin A, Sanzey M, Rahim SA, Fack F, et al. Anti-VEGF treatment reduces blood supply and increases tumor cell invasion in glioblastoma. Proc Natl Acad Sci USA 2011; 108: 3749–54.

Klink B, Schlingelhof B, Klink M, Stout-Weider K, Patt S, Schrock E. Glioblastomas with oligodendroglial component - common origin of the different histological parts and genetic subclassification. Anal Cell Pathol 2010; 33: 37–54.

Klopp AH, Gupta A, Spaeth E, Andreeff M, Marini F III. Concise review: dissecting a discrepancy in the literature: do mesenchymal stem cells support or suppress tumor growth? Stem Cells 2011; 29: 11–9.

Mouthon MA, Fouchet P, Mathieu C, Sii-Felice K, Etienne O, Lages CS, et al. Neural stem cells from mouse forebrain are contained in a population distinct from the 'side population'. J Neurochem 2006; 99: 807–17.

Najbauer J, Huszthy PC, Barish ME, Garcia E, Metz MZ, Myers SM, et al. Cellular host responses to gliomas. PLoS One 2012; 7: e35150.

Niclou SP, Danzeisen C, Eikesdal HP, Wiig H, Brons NH, Poli AM, et al. A novel eGFP-expressing immunodeficient mouse model to study tumor-host interactions. FASEB J 2008; 22: 3120–8.

Ogden AT, Waziri AE, Lochhead RA, Fusco D, Lopez K, Ellis JA, et al. Identification of A2B5 + CD133- tumor-initiating cells in adult human gliomas. Neurosurgery 2008; 62: 505–14, discussion 514–5.

Park DM, Rich JN. Biology of glioma cancer stem cells. Mol Cells 2009; 28: 7–12.

Patrawala L, Calhoun T, Schneider-Broussard R, Zhou J, Claypool K, Tang DG. Side population is enriched in tumorigenic, stem-like cancer cells, whereas ABCG2 + and ABCG2- cancer cells are similarly tumorigenic. Cancer Res 2005; 65: 6207–19.

Reardon DA, Desjardins A, Rich JN, Vredenburgh JJ. The emerging role of anti-angiogenic therapy for malignant glioma. Curr Treat Options Oncol 2008; 9: 1–22.

Sakariassen PO, Prestegarden L, Wang J, Skaftnesmo KO, Mahesparan R, Molthoff C, et al. Angiogenesis-independent tumor growth mediated by stem-like cancer cells. Proc Natl Acad Sci USA 2006; 103: 16466–71.

Schinkel AH. P-Glycoprotein, a gatekeeper in the blood-brain barrier. Adv Drug Deliv Rev 1999; 36: 179–94.

Schulte A, Gunther HS, Martens T, Zapf S, Riethdorf S, Wulfing C, et al. Glioblastoma stem-like cell lines with either maintenance or loss of high-level EGFR amplification, generated via modulation of ligand concentration. Clin Cancer Res 2012; 18: 1901–13.

Seidel S, Garvalov BK, Wirta V, von Stechow L, Schanzer A, Meletis K, et al. A hypoxic niche regulates glioblastoma stem cells through hypoxia inducible factor 2 alpha. Brain 2010; 133: 983–95.

Singh SK, Clarke ID, Terasaki M, Bonn VE, Hawkins C, Squire J, et al. Identification of a cancer stem cell in human brain tumors. Cancer Res 2003; 63: 5821–8.

Singh SK, Hawkins C, Clarke ID, Squire JA, Bayani J, Hide T, et al. Identification of human brain tumour initiating cells. Nature 2004; 432: 396–401.

Son MJ, Woolard K, Nam DH, Lee J, Fine HA. SSEA-1 is an enrichment marker for tumor-initiating cells in human glioblastoma. Cell Stem Cell 2009; 4: 440–52.

Szotek PP, Pieretti-Vanmarcke R, Masiakos PT, Dinulescu DM, Connolly D, Foster R, et al. Ovarian cancer side population defines cells with stem cell-like characteristics and Mullerian Inhibiting Substance responsiveness. Proc Natl Acad Sci USA 2006; 103: 11154–9.

Tang DG. Understanding cancer stem cell heterogeneity and plasticity. Cell Res 2012; 22: 457–72.

Torok M, Huwyler J, Gutmann H, Fricker G, Drewe J. Modulation of transendothelial permeability and expression of ATP-binding cassette transporters in cultured brain capillary endothelial cells by astrocytic factors and cell-culture conditions. Exp Brain Res 2003; 153: 356–65.

Wang J, Miletic H, Sakariassen PO, Huszthy PC, Jacobsen H, Brekka N, et al. A reproducible brain tumour model established from human glioblastoma biopsies. BMC Cancer 2009; 9: 465.

Wang J, Sakariassen PO, Tsinkalovsky O, Immervoll H, Boe SO, Svendsen A, et al. CD133 negative glioma cells form tumors in nude rats and give rise to CD133 positive cells. Int J Cancer 2008; 122: 761–8.

Wu C, Alman BA. Side population cells in human cancers. Cancer Lett 2008; 268: 1–9.

Wu C, Wei Q, Utomo V, Nadesan P, Whetstone H, Kandel R, et al. Side population cells isolated from mesenchymal neoplasms have tumor initiating potential. Cancer Res 2007; 67: 8216–22.

Zhou S, Schuetz JD, Bunting KD, Colapietro AM, Sampath J, Morris JJ, et al. The ABC transporter Bcrp1/ABCG2 is expressed in a wide variety of stem cells and is a molecular determinant of the side-population phenotype. Nat Med 2001; 7: 1028–34.